Journal of the European Ceramic Society 7 (1991) 125–132

Silicon Nitride Oxidation/Re-oxidation

P. Andrews & F. L. Riley*

Division of Ceramics, School of Materials, University of Leeds, Leeds LS2 9JT, UK

(Received 9 July 1990; revised version received 25 October 1990; accepted 5 November 1990)

Abstract

A magnesium- and yttrium-containing sintered silicon nitride was oxidised in air at 1350°C and, after removal of the surface oxide film, re-oxidised. The rates of product formation during the oxidation and re-oxidation stage can be satisfactorily described in terms of oxygen diffusion through a thin protective cristobalite film at the nitride–silicate interface, the inwards diffusion of cations and the sequential reaction of the cristobalite to form silicates providing a lesser degree of protection.

Magnesium- und Yttriumhaltiges gesintertes Si_3N_4 wurde in Luft bei 1350°C oxidiert und nach dem Entfernen der Oxidschicht einer zweiten Oxidationsbehandlung unterzogen. Die Geschwindigkeiten der Schichtbildung während der zweiten Oxidation können gut durch die Sauerstoffdiffusion durch eine schützende dünne Cristobalit-Schicht an der Nitrid–Silikat-Grenzfläche und eine nachfolgende Umwandlung des Cristobalits zu Silikaten mit einer reduzierten Schutzwirkung beschrieben werden.

On a oxydé à 1350°C dans l'air du nitrure de silicium fritté contenant du magnésium et de l'yttrium puis, après avoir enlevé le film surfacique d'oxyde, on a réoxydé le matériau. Les vitesses de formation du produit lors de l'étape de réoxydation peuvent être décrites de manière satisfaisante en termes de diffusion d'oxygène à travers un film protecteur mince de cristobalite à l'interface nitrure–silicate, la réaction ultérieure de la cristobalite conduisant à la formation de silicates fournissant un degré de protection moindre.

* To whom correspondence should be addressed.

1 Introduction

Silicon nitride based ceramics require metal oxide additives to ensure high sintered density. Densification of silicon nitride powder occurs through a liquid-phase sintering process, the liquid silicates generally being formed by reactions between the additive and the natural surface silicon dioxide on the silicon nitride particles. On cooling the liquid solidifies to form an intergranular phase, which can be amorphous or crystalline, depending on the system, the starting composition within that system, and the heat treatment. The presence of intergranular material, and more specifically its cation content, is believed to have a strong influence on the external oxidation behaviour of dense (sintered or hot-pressed) silicon nitride.[1] Under conditions of high oxygen potential, such as air or oxygen at 1 bar, silicon nitride materials oxidise at rates which normally decrease with time. The more detailed kinetic behaviour depends on the composition of the material and in some cases also on the temperature. A parabolic relationship tends to be followed fairly accurately and irrespective of temperature for materials containing a significant proportion of magnesium oxide.[2,3] Where yttrium oxide has been used as a densification aid approximately logarithmic, or more complex, relationships can appear to provide better fits to experimental data,[4] although parabolic behaviour has also been reported.[5] The oxide films produced always contain, in the form of crystalline or glassy silicates, cations originally present in the silicon nitride intergranular phase.[6,7] Where parabolic kinetics are observed, diffusion control of oxidation is commonly assumed and, because the underlying silicon nitride may show a marked cation concentration gradient, this leads

Journal of the European Ceramic Society 0955-2219/91/$3.50

naturally to the conclusion that the outward diffusion of cations (and counter-balancing anions) may be the rate-controlling process.[8] In other cases where, for example, aluminium and yttrium oxides have been the major densification aids, workers have assumed that the oxidation product is protective and that the rate-controlling process is the inward diffusion of oxygen through a dense, partially crystalline, silicate film.[9] Changes in oxidation behaviour are then correlated with, for example, changes in film structure or in glass or liquid viscosity.

Recently a detailed examination of the high-temperature oxidation behaviour in air of a silicon nitride densified with magnesium and yttrium oxides has been made, for which the kinetics were closely parabolic.[10] The study led to the conclusion that a combination of two primary diffusion processes may control the overall oxidation rate. The first process is the inward diffusion of oxygen through a thin surface film of cristobalite; the second is the outward diffusion of intergranular metal oxide or its equivalent, which reacts with the cristobalite film to form the corresponding silicates. This model is based on the recognition that a major component of the oxidation reaction is the formation of metal silicates in the oxide film, and thus the partial loss of potentially protective cristobalite.

The oxidation of silicon nitride materials is generally predominantly external, as has been assumed in the preceding paragraph, but a degree of simultaneous internal oxidation can occur. The exaggerated effects of this can be seen dramatically in materials densified with yttrium oxide and containing intergranular quaternary silicon yttrium nitride oxides. Oxidation of these quaternary nitrides is associated with large volume expansions, which are believed to be responsible for mechanical disruption of the intergranular regions, and consequent complete loss of strength of the material.[11] The kinetics of oxidation under these conditions can be approximately linear, since a protective oxide film is not formed.

Material densified with magnesium oxide can also show a more restrained and less degrading internal oxidation, particularly after extended times, with the appearance of intergranular silicon oxynitride[12] (the strain induced by the ~20% volume expansion associated with the oxidation of silicon nitride to silicon oxynitride must then presumably be adequately accommodated by the system). The internal oxidation process may involve the simple inward diffusion of oxygen into an intergranular glass, but it has also been modelled for magnesium-containing silicon nitrides in terms of an intergranular phase–surface silicon dioxide interaction which can be regarded as a reaction between silicon nitride and intergranular magnesium-containing silicate to form silicon oxynitride,[13] and the release of nitride ion to the surface. Nitrogen gas is formed in the surface layer by oxidation to the nitride ion, with simultaneous release of oxide ions to form external silicate. These reactions can be regarded as:

$$3MgSiO_{3(\text{intergranular glass})} + 5Si_3N_4 = Mg_3N_2 + 9Si_2N_2O \quad (1)$$

$$Mg_3N_2 + 3SiO_{2(\text{surface})} + 1\tfrac{1}{2}O_2 = 3MgSiO_{3(\text{surface})} + N_2 \quad (2)$$

Commonly, however, the oxynitride is only seen in a very thin sub-surface layer of the silicon nitride, and most of the oxidation mass gain of a sintered silicon nitride can be accounted for by the external oxidation of silicon nitride to silicon dioxide. This was the case for the magnesium and yttrium oxide densified material used in the present study.

Important evidence that the surface oxide film may not be protective, and that the outward flow of intergranular phase cations could thus be rate-controlling, was first provided by the oxidation/re-oxidation experiments of Cubicciotti & Lau.[14] A magnesium oxide densified silicon nitride was oxidised and the oxide film was then removed by grinding, before continuing oxidation under identical conditions. The mass-gain curve for re-oxidation was a close fit to a continuation of the original parabola, rather than the repeated initial stage parabola which would have been expected from a protective surface oxide film with rate control by the inward diffusion of oxygen through the film.

The oxidation/re-oxidation experiment has been used in many subsequent studies of the oxidation mechanisms of other silicon nitride based materials, formed with a range of densification additives, and with various oxidation temperatures and times. Three types of re-oxidation kinetics can be distinguished:

(1) An uninterrupted close continuation of the original parabola;
(2) initially slightly faster than that at the termination of oxidation, but slower than the initial rate in the oxidation period;
(3) a repeat of the first oxidation period.

A summary of data is given in Table 1.

In the first case re-oxidation rates are apparently independent of the surface oxide film thickness, and the outward diffusion of cations might be assumed

Table 1. Classification of types of silicon nitride re-oxidation kinetics, and the sintering additives used

Type	*Additive*	*Reference*
1	MgO	14
	Al_2O_3 and CaO	15
	Al_2O_3	16
	MgO	17
	MgO	18
2	Y_2O_3	18
	Y_2O_3-containing systems	17
3	CeO_2	19

to be the rate-controlling step. In the second, a degree of protection can be attributed to the oxide film, but the rate of oxidation appears to be largely controlled by some process not involving diffusion through the oxide film. In the third case, inward oxygen diffusion through the oxide film appears to control oxidation.

The present authors' detailed investigation[10] into the oxidation of a silicon nitride sintered with a combination of magnesium and yttrium oxides provides the basis for a model which assumes that the essential function of the intergranular-phase cations (and associated charge-balancing anions) is to modify the thickness of a thin, but potentially protective, cristobalite layer forming at the interface between the silicon nitride and the outer silicate layer. The oxidation rate-controlling process is thus the sequential inward diffusion of oxygen (to generate silicon dioxide), and the outward diffusion of intergranular metal oxide as a result of ionic chemical potential gradients (to convert silicon dioxide to silicate). It is assumed that oxygen mobility in the silicate is greater than that in cristobalite.

A series of oxidation/re-oxidation experiments has now been carried out to test whether the model permits predictions of re-oxidation rate and cristobalite film thickness. In principle, if the rate constants controlling cristobalite formation and its reaction to form silicate are known, it is a simple matter to simulate by computer the consequences of removing the cristobalite layer, and then allowing oxidation to continue.

2 Experimental

A sintered reaction-bonded silicon nitride (SRBSN) designated 10.2.2 by the suppliers (British Ceramic Research Laboratories, Stoke-on-Trent, UK) was used. This designation refers to the sintering additive composition of 10% Y_2O_3, 2% MgO and 2% Cr_2O_3 (by mass), which gives approximate molar proportions of 7:7:2. According to the suppliers the three oxides were mixed with silicon powder which was then compacted, nitrided and finally sintered to full density using the standard powder bed method. Further details of the preparation route and material are given in a patent application.[20]

The SRBSN was supplied as a tile $\sim 150\,mm \times 150\,mm \times 12\,mm$. A minimum of 1·5 mm was ground from all surfaces to remove a layer of material which showed significant structural differences compared with the interior. Samples, $\sim 4\,mm \times 4\,mm \times 8\,mm$, were cut from the tile and prepared for oxidation by grinding with 400 mesh silicon carbide powder, followed by ultrasonic cleaning under acetone. The density of the material, as measured by mercury immersion, was $3{\cdot}22\,Mg\,m^{-3}$.

Oxidation was carried out in a vertical tube furnace, at $1350 \pm 5°C$ in an atmosphere of flowing laboratory air ($1{\cdot}5\,cm^3\,s^{-1}$). The oxidation rate was followed by intermittently withdrawing the sample and weighing to $\pm 10\,\mu g$. Mass change data were normalised to mass gain per unit area of surface ($\Delta m/A$). After 85 ks the oxide film was carefully removed from the surface by scraping with a piece of unoxidised SRBSN followed by gently grinding with 1000 mesh SiC powder. Measurements of the change in mass of the sample after it had been scraped, and during grinding, were used to monitor the amount of oxide removed. The sample was then re-oxidised under the same conditions for a further 85 ks, with continued intermittent measurements of mass change.

Sample surfaces were intermittently examined under standardised conditions using X-ray diffraction analysis (XRD) during the oxidation and the re-oxidation processes. To allow for partial absorption of the X-ray beam by the surface silicate film, oxidation product peak-height values were adjusted using a semi-empirical correction factor obtained on the basis of the reduction in intensities of selected major β-Si_3N_4 peaks of the oxidised material, by comparison with those obtained under identical conditions from the surface of unoxidised material. The molar proportions of the three crystalline products in the oxide film, α-cristobalite, protoenstatite and γ-yttrium disilicate, were then calculated from the corrected XRD peak heights, on the basis of conversion graphs constructed using the XRD peak heights of mixtures of known composition of the three phases. These standard mixtures were prepared from the three-component binary

oxides by equilibration at 1300°C for 85 ks, followed by quenching to room temperature and powdering. The eutectic temperature in this sub-system is ~1385°C,[10] and the equilibrated phase composition thus depends only on the proportions of the components used. The diffraction peaks used for these analyses were α-cristobalite (101), proto-enstatite (220), (310), (102), γ-$Y_2Si_2O_7$ (121), (111), (210) and β-Si_3N_4 (200), (101), (210).

3 Results

The means of three sets of oxidation/re-oxidation data are presented as plots of Δm/A and of $(\Delta m/A)^2$ as functions of time in Figs 1 and 2. Oxidation shows clear parabolic behaviour, whereas the re-oxidation does not. Over the time period studied the re-oxidation was slower than that of the initial oxidation, but slightly faster than that which would have given a continuation of the first parabola. The form of the $(\Delta m/A)^2$–time relationship suggests that prolonged re-oxidation might eventually lead to re-establishment of the first stage oxidation parabola.

XRD surface analyses carried out under standardised conditions showed the presence of α-cristobalite, proto-enstatite and γ-yttrium disilicate. The underlying β-silicon nitride was the only other crystalline phase detected and its XRD peaks became progressively weaker with increasing time of oxidation. Calibration curves[10] were used to obtain a measure of the amount of each crystalline phase present in the oxide film. This amount is expressed in terms of a quantity Q_i, the product of the corrected and summed XRD peak heights ($\sum I_i$) for that phase (i) and a conversion factor (f_i) relating summed peak height to (molar) proportion of the phase present in a mixture of the three. Oxide film compositions during oxidation and re-oxidation as a function of time at 1350°C are shown in Fig. 3. The curves drawn for the oxidation period are the best-fit parabolas for the data up to 60 ks.

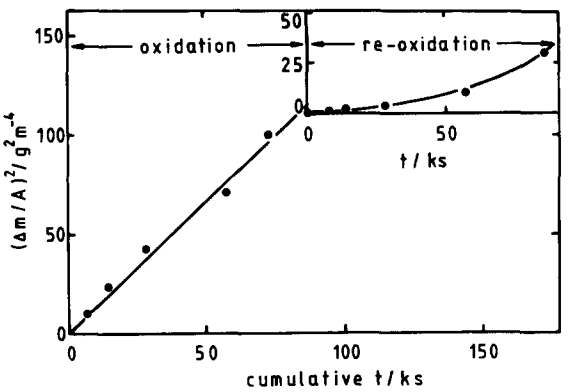

Fig. 2. Data from Fig. 1 plotted in parabolic form.

During oxidation the formation of all three phases in the film closely follows parabolic kinetics (consistent with the mass gains obtained) although the formation of cristobalite shows a more marked decrease after ~60 ks.

At the end of the first oxidation period proto-enstatite is the major component of the oxide film, with much smaller amounts of α-cristobalite at the nitride–silicate interface and of γ-yttrium disilicate near the silicate–air interface.[10]

During re-oxidation the rates of formation of the two crystalline silicates do not fit parabolic kinetics, although the rate of formation of cristobalite is still closely parabolic, but slightly faster than the oxidation stage rate. This effect is shown clearly in the ratio of $(Q_{silicate}/Q_{cristobalite})$, which in the first oxidation period is much larger than that of the initial stage of re-oxidation (Fig. 4). The horizontal line drawn is the best fit through the first three points, in recognition of the departure (Fig. 3) of the cristobalite curve from parabolic form after ~60 ks, and which would have the effect of increasing the

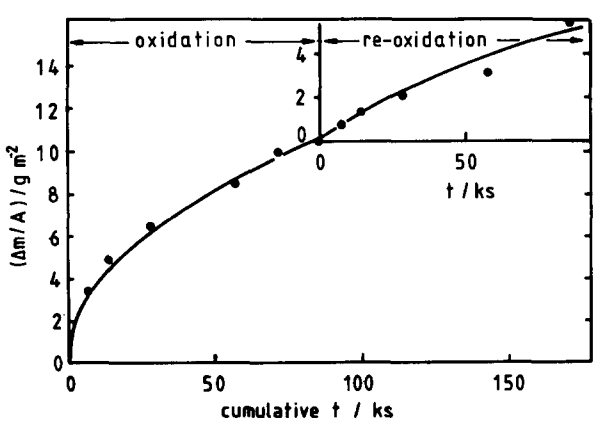

Fig. 1. Mass gain per unit area as a function of oxidation and re-oxidation time at 1350°C.

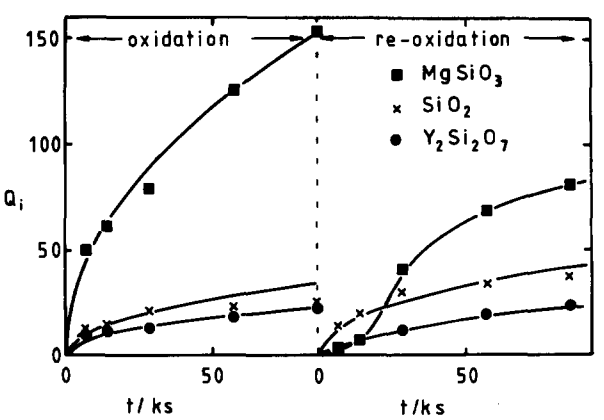

Fig. 3. Oxide film composition (Q_i) as a function of oxidation and re-oxidation time.

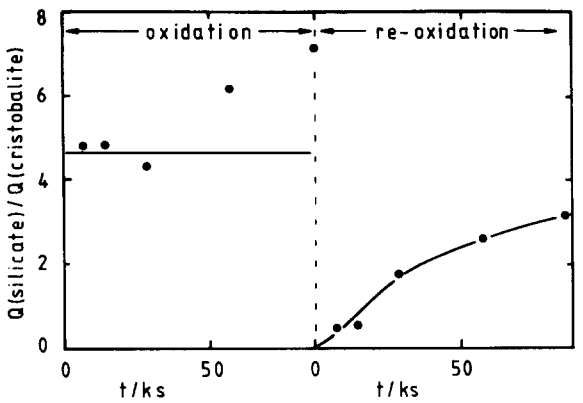

Fig. 4. Oxide film composition, expressed as the ratio (quantity of silicate)/(quantity of cristobalite), as a function of oxidation and re-oxidation time.

silicate/cristobalite ratio for enstatite and yttrium disilicate. The steady and marked shift in the ratio with increasing time of re-oxidation suggests that a ratio corresponding to that of the first oxidation period might eventually be re-established.

4 Discussion

The earlier detailed study[10] showed that in this system at temperatures below the oxide product eutectic temperature of 1385°C a thin layer of cristobalite is developed at the nitride–silicate interface. Oxygen diffusion in cristobalite (the β-phase at high temperature) is very slow compared with that in silicate glasses.[21] Inward diffusion of oxygen through the cristobalite layer will therefore be an important factor controlling the oxidation rate, and any process influencing the thickness of the crystobalite layer must also control the oxidation rate. A major component of the oxidation process, shown clearly by Fig. 3, is the extensive reaction between cristobalite and metallic (and oxide) ions diffusing from the intergranular phase to form magnesium and yttrium silicates. The protective layer of cristobalite cannot therefore develop as effectively as would be the case in the absence of the intergranular-phase material.

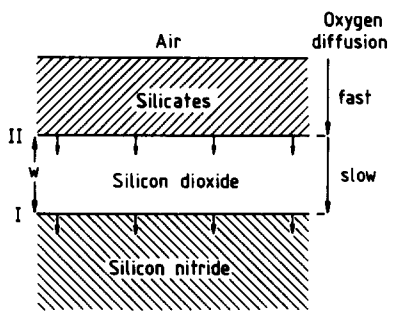

Fig. 5. Schematic representation of the silicon nitride oxidation process, with simultaneous formation of silicon dioxide at interface I and its reaction to form silicate at interface II.

The model for the overall oxidation process, in which cristobalite is simultaneously formed by oxidation of silicon nitride, and consumed by reaction with (effectively) metal oxide to form a silicate is shown schematically in Fig. 5. Oxidation is postulated to be controlled by the rate of permeation of oxygen through a thin cristobalite film, the thickness (w) of which is determined by the two factors:

(1) The rate of formation by oxidation of the silicon nitride:

$$\frac{dw}{dt} = \frac{\alpha}{w} \tag{3}$$

where α is an experimental rate constant;

(2) the reaction with metal oxide to form a silicate:

$$-\frac{dw}{dt} = \beta . t^{-1/2} \tag{4}$$

The silicate-forming reaction, summarised in eqn (4), is assumed also to follow parabolic kinetics, on the basis that its rate is determined by the rate of diffusion of metal oxide (or the ionic equivalents) from the silicon nitride intergranular region, with an experimental rate constant β. The overall rate of increase of thickness of the cristobalite layer (dw/dt) is therefore:

$$\frac{dw}{dt} = \frac{\alpha}{w} - \beta . t^{-1/2} \tag{5}$$

and

$$w = [(\beta^2 + 2\alpha)^{1/2} - \beta] . t^{1/2} \tag{6}$$

The observed oxidation rate is:

$$\frac{dP}{dt} = \frac{\alpha}{[(\beta^2 + 2\alpha)^{1/2} - \beta]} . t^{-1/2} \tag{7}$$

and if $P = 0$ at $t = 0$, then

$$P = \frac{2\alpha}{[(\beta^2 + 2\alpha)^{1/2} - \beta]} . t^{1/2} \tag{8}$$

where P is proportional to the distance moved by the nitride–oxide interface into the silicon nitride, and thus to the recorded oxidation mass gain.

The value of β is related to the outward diffusion of cations from the intergranular phase, and can readily be determined from the observed rates of formation of silicate, in this case crystalline enstatite and yttrium disilicate. The value for α is obtained from the measured oxidation mass gain, and the

calculated value of β, using eqn (8). Mean values of α and β are $4{\cdot}7 \times 10^{-16}\,m^2\,s^{-1}$ and $2{\cdot}8 \times 10^{-8}\,m\,s^{-1/2}$ respectively for oxidation at 1350°C, on the basis of mass gain and XRD analysis datum points for the first oxidation stage. These are close to the values of $2{\cdot}9 \times 10^{-16}\,m^2\,s^{-1}$ and $2{\cdot}5 \times 10^{-8}\,m\,s^{-1/2}$ previously reported.[10]

It must be noted that because this method for determining β, and thus α, rests on XRD data, any silica or silicate glass will be ignored and a possible source of error exists. SEMs of oxide films (including dot-mapping) show, however, that the bulk of the surface film is crystalline, and visually accounted for by the presence of the three crystalline phases indicated by the XRD patterns. While there is no obvious glass phase, the presence of small amounts certainly cannot be ruled out; it is not considered likely, however, that the values of α and β will be seriously in error.

Use of the detailed XRD data for the product oxides permits calculation of the amounts of each of the three phases in the oxide film. This is readily carried out on the basis of the total amount of silicon dioxide generated, which is obtained immediately from the mass gain data, since:

$$Si_3N_4 + 3O_2 = 3SiO_2 + 2N_2 \qquad (9)$$

and a mass gain of $1\,g\,m^{-2}$ corresponds to the formation of $4{\cdot}51\,g\,m^{-2}$ of silicon dioxide, and the proportions (Q_i) in molar terms of cristobalite, enstatite and yttrium disilicate obtained from the XRD data. The amount of each phase present is for convenience converted also into film thickness of the phase, using standard density values, and assuming that each phase is present as a uniform thin film (which in fact is not far from the actual case).

The values of α and β derived from the oxidation mass gain and XRD peak height data have been used to generate theoretical mass gain and product film thickness curves for the oxidation and re-oxidation processes. For the re-oxidation stage it is assumed that all the cristobalite has been removed from the silicon nitride surface, thus resetting w to zero. The time axis is continuous, since this represents the uninterrupted flow of metal oxide from the intergranular phase, and thus the smooth continuation of process (4).

Oxidation and re-oxidation data are shown in standard parabolic form in Fig. 6, in which the points correspond to the derived total thickness of the oxide film as a function of time, and the curves drawn are those calculated using the α and β values. The computed line for the oxidation stage fits well all the experimental points, indicating that there is no

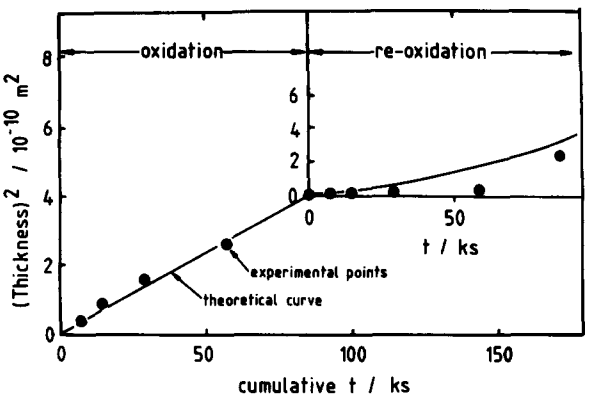

Fig. 6. Oxide film thickness (squared) as a function of time during oxidation and re-oxidation. The lines are those calculated on the basis of the experimental α and β values.

significant drift in the rate constants with oxidation time (and build-up of product film thickness). The re-oxidation curve has the same overall form as the experimental curve, with initial values of oxidation rate being slightly lower than those predicted on the basis of the first-stage oxidation behaviour. The overall good agreement, however, confirms the applicability of the model.

Computed data for the silicate film thickness as a function of time are shown in Figs 7 and 8. Because the silicates are the major products these curves also have the same overall form as that of the corresponding mass gain curve (Figs 1 and 2). An important difference, however, is that the curve describing the silicate film thickness gives a continuation of the original parabola, whereas the mass gain curve does not. Figure 9 shows the computed curves for the cristobalite film thickness during oxidation and re-oxidation, and the experimental datum points. Although the curves have the same form, the experimental cristobalite film thicknesses are uniformly a factor of 1·8 larger than those predicted. This is possibly the result of

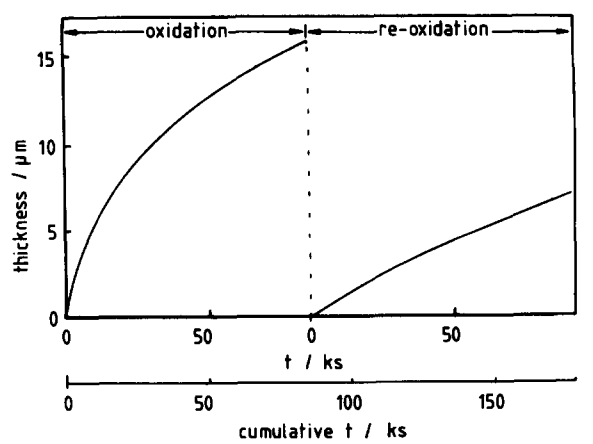

Fig. 7. Computed total oxide film thickness as a function of time during oxidation and re-oxidation.

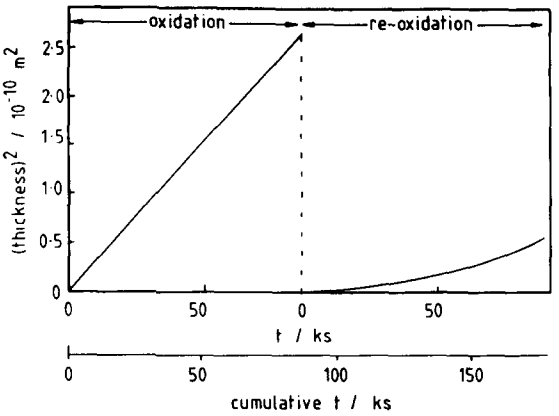

Fig. 8. Computed total oxide film thickness (squared) as a function of time during oxidation and re-oxidation.

systematic errors in calculating the proportion of cristobalite present in the oxide film. The cristobalite always lies at the nitride–silicate interface, magnifying the effects of small errors in the peak-height correction factor. It is likely that slight systematic errors will also be attached to calculation of the proportions of enstatite and yttrium disilicate present in the film, because of the influence of crystal preferred orientation on peak intensity. The use of summed intensities from these peaks in each case would, however, be expected to alleviate this problem to some extent. This also means that the calculated values of α and β have a similarly based error attached to them, but the broad qualitative picture is not changed. The rapid increase in cristobalite yield at commencement of re-oxidation, by comparison with that of the uninterrupted oxidation, is explained by the loss of protection to the silicon nitride, and the now reduced flux of metal oxide as a result of the depletion of the intergranular phase material, and hence decreased chemical potential gradient.

It is instructive to examine the consequences of accidentally, and probably unavoidably, removing some unoxidised silicon nitride during removal of

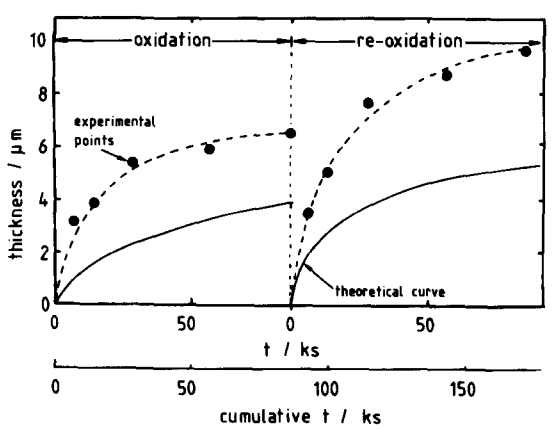

Fig. 9. Cristobalite film thickness as a function of time during oxidation and re-oxidation.

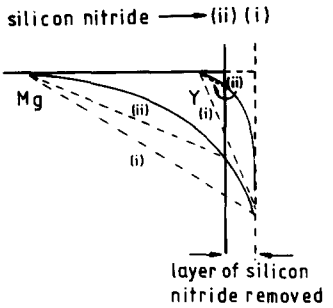

Fig. 10. Schematic representation of the changing chemical potential gradient of Mg^{2+} and Y^{3+} (vertical axis) with distance from the silicon nitride surface, before (i) and after (ii) removal of a thin silicon nitride film. The concentration gradient is most disturbed in the Y^{3+} case.

the surface oxide film prior to re-oxidation. This is shown schematically in Fig. 10. Because Mg^{2+} is $\sim 2{\cdot}5$ times more mobile in the intergranular phase than Y^{3+} (seen clearly in the preponderance of enstatite in the product film),[10] the Mg^{2+} chemical potential gradient will be shallower that that of Y^{3+}. The removal of an outer layer of silicon nitride will have a less marked effect on the Mg^{2+} chemical potential gradient existing at the commencement of re-oxidation by comparison with that of Y^{3+}. In these experiments the proportion of yttrium disilicate formed on re-oxidation was greater than that for oxidation, consistent with some loss of silicon nitride together with sub-surface intergranular metal oxide, and giving a consequently increased relative flux of Y^{3+}.

Examination of the earlier data for oxidation/re-oxidation experiments shows a similar pattern, and the probable effect of the accidental removal of some unoxidised silicon nitride (and thus some intergranular metal oxide) during preparation for the re-oxidation stage. There is a clear tendency for the re-oxidation stage to be slightly faster than the projected continuation of the oxidation curve, which is now explained by the loss of protective cristobalite. This tendency is, however, most marked in the case of materials densified with the less mobile Y^{3+} (and possibly the also highly charged Ce^{3+}) ions. This is as would be expected, because the underlying metal oxide chemical potential gradient is most disturbed by the loss of a thin layer of silicon nitride in these cases. With the slower moving ions, loss of surface silicon nitride is equivalent, in the limit, to restarting the oxidation process from $t = 0$.

5 Conclusions

The application to the silicon nitride re-oxidation experiment of a model which assumes that oxidation

is controlled by the diffusion of oxygen through a developing surface film of cristobalite which is simultaneously reacting with metal oxide to form silicates, gives mass gain and product composition data which are in good agreement with experimentally determined values. It appears that the oxidation rate of this multiphase silicon nitride material is controlled by a thin surface film of cristobalite. The stability of this film is controlled by the type and availability of silicon nitride intergranular phase cations. Intergranular phase Mg^{2+} is more mobile than Y^{3+}, and with the mixed additive system of this material, the oxidation product is predominantly enstatite. Metal ion chemical potential gradients between the silicon nitride intergranular phase and the silicon dioxide surface film tend to be shallower for Mg^{2+} than for Y^{3+}, and the effects of the removal of a layer of silicon nitride with surface oxide in preparing for re-oxidation are therefore less marked. An interpretation of the results of previous oxidation/re-oxidation experiments is obtained in these terms.

Acknowledgements

This work was supported by an SERC CASE Studentship. Rolls Royce plc assisted with the supply of materials, and E. Gilbart and J. H. Merkin are thanked for very helpful discussions.

References

1. Billy, M. & Desmaison, J. G., High temperature oxidation of silicon-based structural ceramics. *High Temp. Technol.*, **4**(3) (1986) 131–9.
2. Lange, F. F., Phase relations in the system Si_3N_4–SiO_2–MgO and their inter-relation with strength and oxidation. *J. Am. Ceram. Soc.*, **61**(1–2) (1978) 53–6.
3. Babini, G. N. & Vincenzini, P., Oxidation kinetics of hot-pressed silicon nitride. In *Progress in Nitrogen Ceramics*, ed. F. L. Riley. Martinus Nijhoff, The Hague, 1983, pp. 427–38.
4. Ernstberger, U., Grathwohl, G. & Thümmler, F., High temperature durability and limits of sintered and hot-pressed silicon nitride materials. *Int. J. High Technol. Ceram.*, **3** (1987) 43–61.
5. Bouarroudj, A., Gowsat, P. & Besson, J. L., Oxidation resistance and creep behaviour of a silicon nitride ceramic densified with Y_2O_3. *J. Mat. Sci.*, **20** (1985) 1150–9.
6. Kiehle, A. J., Heung, L. K., Gielisse, P. J. & Rockett, T. J., Oxidation behaviour of hot-pressed silicon nitride. *J. Am. Ceram. Soc.*, **58**(1–2) (1975) 17–20.
7. Tripp, W. C. & Graham, H. C., Oxidation of Si_3N_4 in the range 1300°C to 1500°C. *J. Am. Ceram. Soc.*, **59**(9–10) (1976) 399–403.
8. Singhal, S. C., Oxidation of silicon nitride and related materials. In *Nitrogen Ceramics*, ed. F. L. Riley. Noordhoff, Leyden, 1977, pp. 607–26.
9. Hasegawa, Y., Tanaka, H., Tsutsumi, M. & Suzuki, H., Oxidation behaviour of hot-pressed Si_3N_4 with addition of Y_2O_3 and Al_2O_3. *Yogyo-kyokai-Shi*, **88**(5) (1980) 292–7.
10. Andrews, P. & Riley, F. L., The microstructure and composition of oxide films formed during high-temperature oxidation of a sintered silicon nitride. *J. Eur. Ceram. Soc.*, **5** (1989) 245–56.
11. Lange, F. F., Singhal, S. C. & Kuznicki, R. C., Phase relations and stability studies in the Si_3N_4–SiO_2–Y_2O_3 pseudoternary system. *J. Am. Ceram. Soc.*, **60**(5–6) (1977) 249–52.
12. Clarke, D. R. & Lange, F. F., Oxidation of Si_3N_4 alloys: relation to phase equilibria in the system Si_3N_4–SiO_2–MgO. *J. Am. Ceram. Soc.*, **63**(9–10) (1980) 586–93.
13. Clarke, D., Thermodynamic mechanism for cation diffusion through an intergranular phase: application to environmental reaction with nitrogen ceramics. In *Progress in Nitrogen Ceramics*. ed. F. L. Riley. Martinus Nijhoff, The Hague, 1983, pp. 421–6.
14. Cubicciotti, D. & Lau, K. H., Kinetics of oxidation of hot-pressed silicon nitride containing magnesia. *J. Am. Ceram. Soc.*, **61**(11–12) (1978) 512–17.
15. Chukukere, F. N. & Riley, F. L., Mass transport processes in the oxidation of calcium doped β'-sialon. In *Mat. Sci. Forum*, Vol. 7, ed. R. Freer & P. F. Dennis. Trans. Tech. Publications, Switzerland, 1986, pp. 307–16.
16. Lewis, G. L. & Barnard, P., Oxidation mechanisms in Si–Al–O–N ceramics. *J. Mat. Sci.*, **15** (1980) 443–8.
17. Ernstberger, U., Grathwohl, G. & Thummler, F., Mechanisms and critical temperatures in oxidation and creep of polyphase silicon nitride materials. In *Ceramic Materials and Components for Engines*, ed. W. Bunk & H. Hausner. Verlag Deutsche Keramische Gesellschaft, 1986, pp. 485–94.
18. Cubicciotti, D. & Lau, K. H., Kinetics of oxidation of yttria hot-pressed silicon nitride. *J. Electrochem. Soc.*, **126**(10) (1979) 1723–8.
19. Quackenbush, C. L. & Smith, J. T., Phase effects of Si_3N_4 containing Y_2O_3 or CeO_2. II. Oxidation. *Am. Ceram. Soc. Bull.*, **59**(5) (1980) 533–7.
20. Cotton, J. W. & Swindells, R., European Patent Application, EP 0 107 919, 9 May 1984.
21. Lamkin, M. A. & Riley, F. L., Oxygen diffusion in silicon dioxide and silicate glasses: a review. to be published.